J Mater Sci: Mater Electron (2022) 33:19612–19626

Precursor solution concentration-dependent electrochemical properties of $CoFe_2O_4$ thin films

Vidyadevi A. Jundale[1] and Abhijit A. Yadav[1,*]

[1] *Thin Film Physics Laboratory, Department of Physics, Electronics and Photonics, Rajarshi Shahu Mahavidyalaya (Autonomous), Latur 413512, Maharashtra, India*

Received: 1 May 2022
Accepted: 20 July 2022
Published online: 2 August 2022

ABSTRACT

$CoFe_2O_4$ thin films have been prepared with various solution concentrations using chemical spray pyrolysis technique. The dependence of precursor solution concentration on physical and electrochemical properties of $CoFe_2O_4$ thin films has been studied. XRD study showed spinel cubic crystal structure symmetry. FESEM micrographs showed mesoporous, spherical grain-like surface morphology. EDAX analysis confirmed formation of stoichiometric $CoFe_2O_4$ thin films. $CoFe_2O_4$ thin films showed high absorption coefficient of 10^4 cm^{-1} with direct allowed type transition and bandgap energies in the range of 2.28–2.45 eV. The $CoFe_2O_4$ thin film prepared with 0.20 M solution concentration showed the lowest electrical resistivity of 2.63 × 10^3 Ωcm and the activation energies in the range of 0.044–0.051 eV and 0.002–0.010 eV. The maximum specific capacitance of 593 Fg^{-1} at scan rate of 5 mVs^{-1} from CV and 628 Fg^{-1} at a current density of 0.5 Ag^{-1} from GCD were observed. The specific energy of 21.97 $Whkg^{-1}$ and specific power of 550 Wkg^{-1} at current density of 2 Ag^{-1} were observed for $CoFe_2O_4$ thin film prepared with 0.20 M solution concentration. Further, the $CoFe_2O_4$ thin film prepared with 0.20 M solution concentration exhibited 92.85% retention of its specific capacitance after 1000 continuous charge–discharge cycles at an applied current density of 1 Ag^{-1}. The electrochemical performance suggests the $CoFe_2O_4$ thin film as a potential electrode material for energy storage applications.

1 Introduction

Spinel ferrites are an extraordinarily useful group of metal oxides with good optical, electronic and magnetic properties. They are auspicious materials to address the sustainable energy conversion and storage as well as the increasing environmental issues [1]. In literature, mostly magnetic and photochemical properties of spinel ferrites have been widely investigated; their electrochemical properties have recently gained attention [2, 3]. Among various ferrites, $CoFe_2O_4$ have low cost, strong anisotropy, excellent chemical and structural stability at high temperature, outstanding electrochemical performance and

Address correspondence to E-mail: aay_physics@yahoo.co.in

https://doi.org/10.1007/s10854-022-08798-2

environment friendliness [4]. These properties make them suitable for various device applications including supercapacitors, transformer cores, microwaves, noise filters, gas sensor and energy storage devices [5].

For the preparation of $CoFe_2O_4$, various techniques are used in literature including co-electrospinning [6], hydrothermal [7], sol–gel [8], electrodeposition [9], chemical vapour deposition [10], co-precipitation [11], spin coating [12], spray pyrolysis [13–15]. Amongst these spray pyrolysis offers excellent advantages such as ease of handling, reasonable cost, large area deposition and ability to produce porous and nanostructured thin films [16, 17].

Previously the $CoFe_2O_4$ thin film electrodes prepared by spray pyrolysis at substrate temperature of 425 °C showed a maximum specific capacitance of 543 Fg^{-1} at scan rate of 5 mVs^{-1} in potential window 0.0 to 0.55 V in aqueous 1 M KOH electrolyte. The maximum specific capacitance, specific energy and specific power from GCD for $CoFe_2O_4$ thin film electrode prepared by spray pyrolysis at substrate temperature of 425 °C were found to be 575 Fg^{-1} at current density of 0.5 Ag^{-1}, 17.85 $WhKg^{-1}$ and 1108.29 Wkg^{-1} at current density of 4 Ag^{-1} respectively. In order to improve the electrochemical performance, $CoFe_2O_4$ thin films were prepared by spray pyrolysis with various solution concentrations. The dependence of precursor solution concentration on the physical and electrochemical properties of has been studied. The results obtained are discussed and compared.

2 Experimental details

$CoFe_2O_4$ thin films were prepared by varying solution concentrations from 0.05 M to 0.25 M at the interval of 0.05 M onto amorphous and FTO coated conducting glass substrates using computerized chemical spray pyrolysis technique at optimized substrate temperature of 425 °C. For the preparation of $CoFe_2O_4$ thin films, AR grade chemicals were used. $Co(NO_3)_2.6H_2O$ and $Fe(NO_3)_3.9H_2O$ were used as precursors. The Co:Fe ratio was kept constant 1:2 for all the depositions. For each deposition, 5 ml $Co(NO_3)_2.6H_2O$ and 10 ml $Fe(NO_3)_3.9H_2O$ were dissolved separately in double distilled water. These precursor solutions were mixed thoroughly by stirring for 15 min and considered as stock solution. 15 ml ethanol was added to stock solution before the depositions. It has been observed that addition of ethanol to stock solution before deposition improves the morphological and electrical properties of $CoFe_2O_4$ thin films significantly. Finally, 30 ml solution was sprayed onto preheated glass and FTO coated conducting glass substrates (7 Ωcm^{-2}). All other parameters were constant at their optimized values namely spray rate; 3–4 $mlmin^{-1}$, substrate to nozzle distance 30 cm; and air as carrier gas with pressure 176,520 Nm^{-2}.

Structural properties and phase identification of $CoFe_2O_4$ thin films were studied using the X-ray diffractometer (Philips model PW-1710) with Cu-Kα radiation (λ = 1.5406 Å). Field emission scanning electron microscope (Model No-S-4800 Hitachi high technologies corporation, Japan) was used to study the surface morphology of $CoFe_2O_4$ thin films. EDAX (Model No-X flash 5030 detector, Bruker AXS Gmbh, Germany) was used to determine the compositions of $CoFe_2O_4$ thin films. To study the optical properties, the optical absorption spectra of $CoFe_2O_4$ thin films was recorded using UV–Vis spectrophotometer (SHIMADZU-1700) within wavelength range of 400 to 800 nm. To determine the electrical resistivity of $CoFe_2O_4$ thin films, DC two-point probe method was used. Electrochemical performances were studied in the standard three-electrode cell on a CHI-608D (CH Instruments, USA). For electrochemical performance, the $CoFe_2O_4$ thin films as a working electrode, platinum (Pt) wire as counter electrode and Ag/AgCl as a reference electrode were used. Initially we tried the different aqueous electrolytes with different concentrations. It has been witnessed that the $CoFe_2O_4$ thin film based supercapacitor showed better electrochemical performance in 1 M KOH electrolyte. Therefore the electrochemical characterizations are performed in 1 M KOH aqueous electrolyte. Using CHI instrument, analysis of cyclic voltammetry (CV) has been carried out at different scan rates within potential range of 0.0 to 0.55 V in 1 M KOH aqueous electrolyte, galvanostatic charge–discharge (GCD) analysis was used to study the charge–discharge behaviour of the $CoFe_2O_4$ electrodes. Using AC signal multi-frequency electrochemical impedance spectroscopy measurement (EIS) was carried out in the frequency range from 1 Hz to 1 kHz.

3 Results and discussion

3.1 Film thickness

Figure 1 shows the photograph $CoFe_2O_4$ thin films prepared by spray pyrolysis with various solution concentrations. It has been observed that the grey colour of $CoFe_2O_4$ thin film changes to black with increase in precursor solution concentration. The colour of $CoFe_2O_4$ thin films varies with film thickness due to light interference phenomena occurring at the metal-oxide-air interfaces. The film thickness of $CoFe_2O_4$ were determined using gravimetric weight difference method [18]. Figure 2 shows the variation of film thickness with solution concentration for $CoFe_2O_4$ thin films prepared by spray pyrolysis. The film thickness increases with increase in solution concentrations initially upto 0.15 M solution concentration and then starts to saturate. This behaviour is due to supply of maximum number of ingredient ($CoFe_2O_4$) ions with increase in solution concentrations. The saturation of the film thickness after 0.15 M solution concentration is due to partial thermal decomposition of the sprayed solution. Similar behavior was reported previously for spray deposited NiO thin films [18].

3.2 X-ray diffraction

The crystal structure of $CoFe_2O_4$ thin films prepared by spray pyrolysis with various solution concentrations was studied using XRD method in 2θ range of 20° to 80°. Figure 3 shows the XRD patterns of the $CoFe_2O_4$ thin films that correspond to (220), (311), (222), (400), (422), (511) and (440) crystallographic planes. All the diffractograms are indexed with standard JCPDS data card (22–1086) to the characteristic reflections of the cubic spinel phase of the Fd-3 m (227) space group [19]. In addition, no other impurity diffraction peaks are witnessed, representing a pure phase formation of $CoFe_2O_4$ thin films by spray pyrolysis. The relative intensity observed for

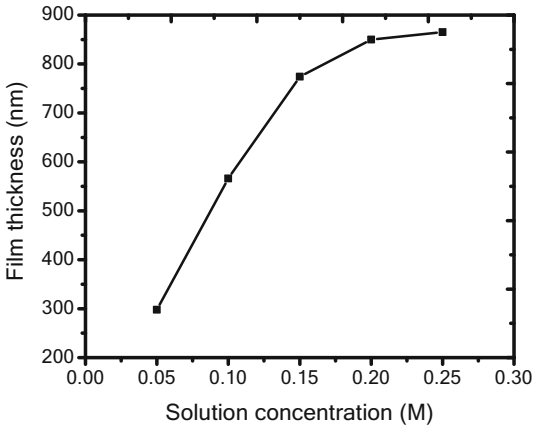

Fig. 2 Variation of film thickness with solution concentration for $CoFe_2O_4$ thin films prepared by spray pyrolysis

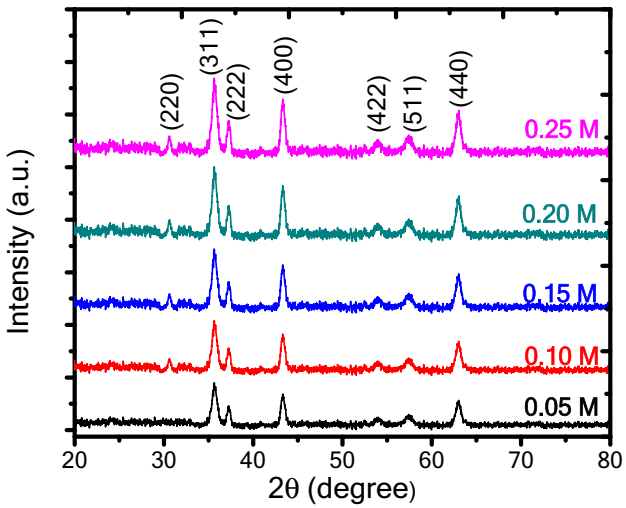

Fig. 3 XRD pattern of $CoFe_2O_4$ thin films prepared by spray pyrolysis at various precursor solution concentrations

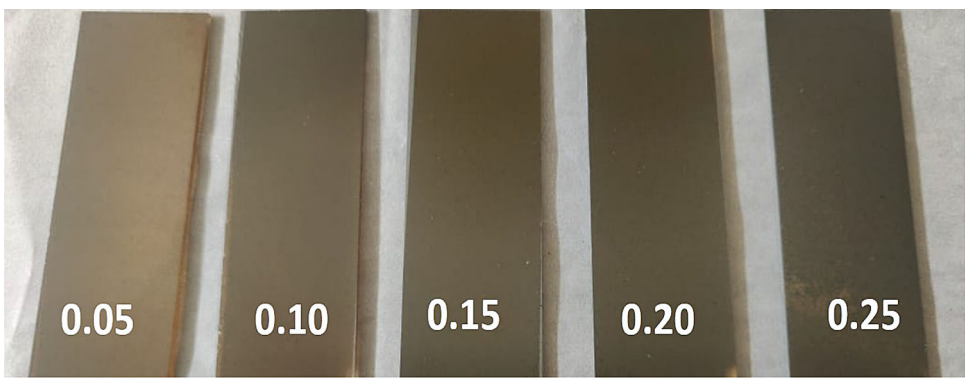

Fig. 1 Photograph of $CoFe_2O_4$ thin films prepared by spray pyrolysis with various precursor solution concentrations

the most prominent peak (311) is increased with increase in as the solution concentration. The probable reason is, at low solution concentration the film thickness is lower and larger grain boundaries per unit area are present in $CoFe_2O_4$ thin films. This leads to strain in film at low solution concentration. With increase in precursor solution concentration, the film thickness increases resulting in reduction in grain boundaries per unit area present in the $CoFe_2O_4$ thin films. Thus, a high extent of crystallization occurs in $CoFe_2O_4$ thin films with increase in precursor solution concentration due to increased film thickness and reduced grain boundaries per unit area present in the $CoFe_2O_4$ thin films. Similar behaviour was previously reported by Babar et al. [20] for sprayed antimony doped tin oxide thin films.

The crystallite sizes of $CoFe_2O_4$ thin films prepared by spray pyrolysis with various solution concentrations were calculated using the Scherer's formula [21]. It is found that, crystallite size of $CoFe_2O_4$ increases with increase in solution concentration from 19 to 29 nm. This is because with increase in precursor solution concentration, the strain and dislocation density are reduced [22]. Similar behaviour of crystallite size has been reported in literature [23, 24]. The lattice parameter 'a' of $CoFe_2O_4$ thin films for (311) plane was determined using the standard relation for cubic phase. The calculated average lattice parameter a = 8.333 Å is close to standard JCPDS data card value a = 8.3910 Å [19]. Table 1 shows the crystallite size, interplanar spacing and lattice constants for $CoFe_2O_4$ thin films prepared by spray pyrolysis with various precursor solution concentrations.

3.3 FESEM

Figure 4 shows the FESEM micrographs (magnification × 200 k) of $CoFe_2O_4$ thin films prepared by spray pyrolysis with various precursor solution concentrations. All the films are crack free, uniform and mesoporous with spherical grain like surface morphology. Surface morphology was observed to be precursor solution concentration dependent. From the FESEM micrographs, one can observe that $CoFe_2O_4$ thin films prepared with solution concentration of 0.05 M (Fig. 4a) shows mesoporous structure. With increase in precursor solution concentration, the mesoporosity increases up to precursor solution concentration of 0.20 M (Fig. 4d). However, with an increase in precursor solution concentration above 0.25 M, the porous structure becomes dense (Fig. 4e) for $CoFe_2O_4$ thin films prepared by spray pyrolysis. Similar mesoporous morphology for $CoFe_2O_4$ thin films was previously reported by Reddy et al. [25] for $CoFe_2O_4$ nanospheres prepared by hydrothermal synthesis and by Shang and colleagues [26] for $CoFe_2O_4$ prepared by nanocasting method. Generally, mesoporous morphology is useful in electrochemical energy conversion and storage devices due to its great potential to achieve high capacitive performance with high specific energy, high specific power, longer lifetime, high interfacial reaction activity and improved kinetics [27].

3.4 EDAX

The chemical purity together with stoichiometry of the $CoFe_2O_4$ thin films was examined by EDAX. Figure 5 shows the EDAX spectra of $CoFe_2O_4$ thin films prepared by spray pyrolysis with various solution concentrations. EDAX spectra shows peaks corresponding to cobalt (Co), iron (Fe) and oxygen (O) elements alone are present in the sample. The EDAX study confirmed that the precursors used for preparation of $CoFe_2O_4$ thin films have completely undergone the chemical effect to form the single-phase nanocrystalline $CoFe_2O_4$. Table 2 shows compositional analysis of $CoFe_2O_4$ thin films prepared by spray pyrolysis with various solution concentrations. It shows that the $CoFe_2O_4$ thin films are nearly homogeneous and stoichiometric.

3.5 Optical

The optical properties of $CoFe_2O_4$ thin films prepared by spray pyrolysis with various precursor solution concentrations were investigated using UV–Vis spectroscopy by measuring the optical absorption spectra in wavelength range 400–800 nm. The absorption spectra were used to study the dependence of precursor solution concentration on the absorption coefficient, bandgap energy and nature of transition (direct or indirect, allowed or forbidden) involved during the absorption process. The absorption coefficient was found to be of the order of 10^4 cm^{-1}. Figure 6a shows the plot of $(\alpha h\upsilon)^2$ against $h\upsilon$ for $CoFe_2O_4$ thin films prepared by spray pyrolysis with various precursor solution concentrations.

Table 1 Structural parameters for $CoFe_2O_4$ thin films prepared by spray pyrolysis with various solution concentrations

Solution Conc. (M)	2θ (°)	d (Å) Obs	d (Å) Std	hkl	a (Å)	D (nm)
0.05	35.58	2.521	2.976	311	8.351	19
	37.16	2.417	2.533	222		
	43.28	2.088	2.097	400		
	53.80	1.702	1.714	422		
	57.38	1.604	1.614	511		
	62.95	1.475	1.482	440		
0.10	30.53	2.925	2.976	220	8.345	21
	35.66	2.515	2.533	311		
	37.13	2.419	2.421	222		
	43.24	2.090	2.097	400		
	53.79	1.703	1.714	422		
	57.22	1.608	1.614	511		
	62.80	1.478	1.482	440		
0.15	30.58	2.921	2.976	220	8.331	23
	35.63	2.517	2.533	311		
	37.20	2.415	2.421	222		
	43.31	2.087	2.097	400		
	53.87	1.700	1.714	422		
	57.40	1.604	1.614	511		
	63.02	1.474	1.482	440		
0.20	30.63	2.916	2.976	220	8.321	27
	35.68	2.514	2.533	311		
	37.28	2.410	2.421	222		
	43.36	2.085	2.097	400		
	53.92	1.699	1.714	422		
	57.45	1.602	1.614	511		
	63.07	1.473	1.482	440		
0.25	30.67	2.912	2.976	220	8.317	29
	35.72	2.511	2.533	311		
	37.29	2.409	2.421	222		
	43.40	2.083	2.097	400		
	53.96	1.698	1.714	422		
	57.51	1.601	1.614	511		
	62.96	1.475	1.482	440		

2θ Bragg's angle, *d* interplanar spacing, *hkl* miller indices, *a* lattice constant, *D* crystallite size

The plot of $(\alpha h\upsilon)^2$ against $h\upsilon$ shows straight line nature indicating direct allowed transition [28, 29] and intercept on energy ($h\upsilon$) axis (x-axis) gives the bandgap energy. Table 3 shows the bandgap energies of $CoFe_2O_4$ thin films prepared by spray pyrolysis with various solution concentrations. These values are in the range of 2.28–2.45 eV and in well agreement with previously reported values [30–32]. From Fig. 6b it has been observed that as precursor solution concentration increases bandgap energy decreases due to thicker films owing to more $CoFe_2O_4$ ions in the film [33]. This may also be related with the increase in crystallinity of $CoFe_2O_4$ films indicating reduction in barrier height at the grain boundaries with enhancement of crystallite size [34]. Similar results has been reported for spray deposited tin oxide thin films with various solution concentrations [33].

3.6 Electrical resistivity

The DC electrical resistivity measurements on $CoFe_2O_4$ thin films were carried out in the temperature range of 300-500 K in the dark. Figure 7 shows the variation of logρ with inverse of absolute temperature (1000/T) for $CoFe_2O_4$ thin films prepared by spray pyrolysis with various precursor solution

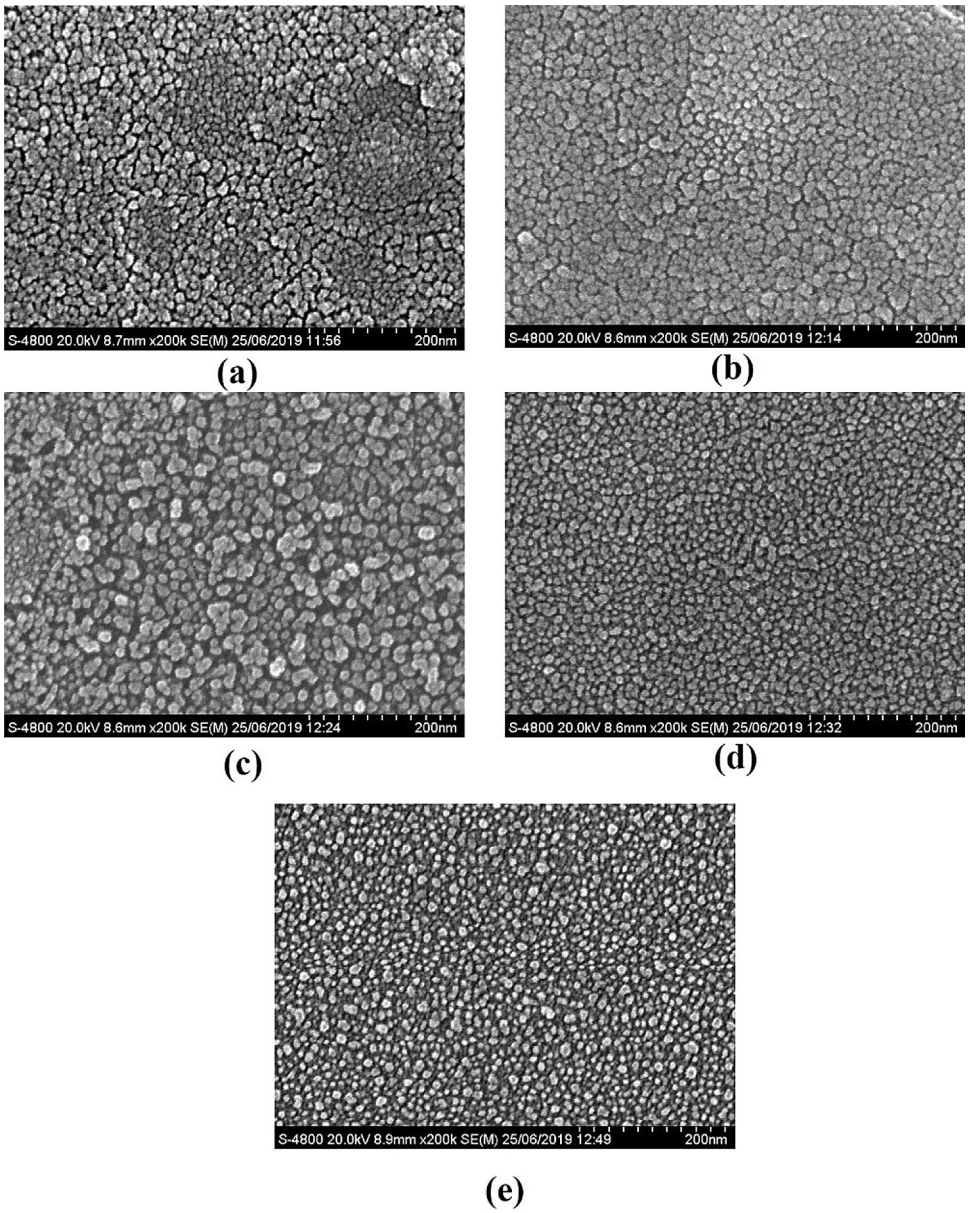

Fig. 4 FESEM images (magnification × 200 k) of $CoFe_2O_4$ thin films prepared by spray pyrolysis with solution concentrations of **a** 0.05 M, **b** 0.10 M, **c** 0.15 M, **d** 0.20 M and **e** 0.25 M, respectively

concentrations. $CoFe_2O_4$ are well-known to be semiconducting material, and this is confirmed by the decreasing electrical resistivity with increase in operating temperature. The electrical resistivity of $CoFe_2O_4$ thin films prepared by spray pyrolysis with various precursor solution concentrations are listed in Table 3. The minimum room temperature electrical resistivity was found to be 2.63×10^3 Ωcm for $CoFe_2O_4$ thin film prepared by spray pyrolysis with precursor solution concentration of 0.20 M. Generally, for ferrite materials electrical resistivity depends on the hopping mechanism in trivalent metal ions in thin film, ionic substitution, film deposition technique and crystal structure of the material [32]. The electrical resistivity of the material also depends on the solution concentrations of trivalent Fe^{3+} ions present in the octahedral A-site and Fe^{3+} and Co^{2+} ions in the tetrahedral B-site [35].

An Arrhenius law dependence of the electrical resistivity of $CoFe_2O_4$ thin films, and the corresponding activation energies (Ea) at low temperature and high temperature regions are given in Table 3. The activation energies were found to be 0.044–0.051 eV and 0.002–0.010 eV in high

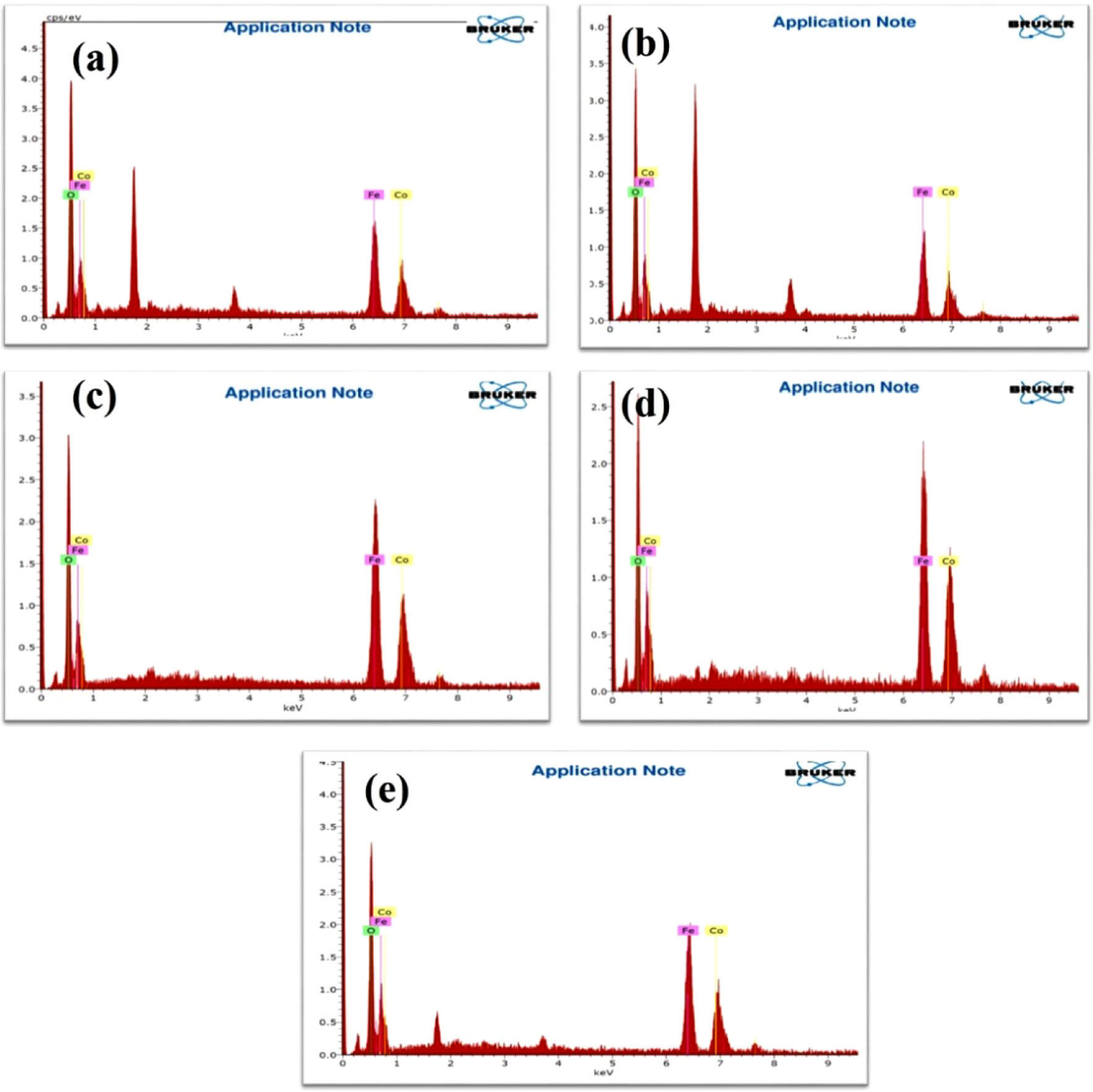

Fig. 5 EDAX spectra of $CoFe_2O_4$ thin films prepared by spray pyrolysis with precursor solution concentrations of **a** 0.05 M, **b** 0.10 M, **c** 0.15 M, **d** 0.20 M and **e** 0.25 M, respectively

Table 2 Compositional analysis of $CoFe_2O_4$ thin films prepared by spray pyrolysis with various precursor solution concentrations

Solution concentration	Atomic percentage in $CoFe_2O_4$ thin films		
(M)	Co	Fe	O
0.05	15.42	29.25	55.33
0.10	15.28	30.02	54.70
0.15	14.34	27.76	57.90
0.20	13.21	29.02	57.77
0.25	13.17	28.95	57.88

temperature and low temperature regions, respectively. The activation energies observed in present study are lower than 0.172 eV reported by Shinde [36] for cobalt ferrite nanopowders obtained by sol–gel auto-combustion method.

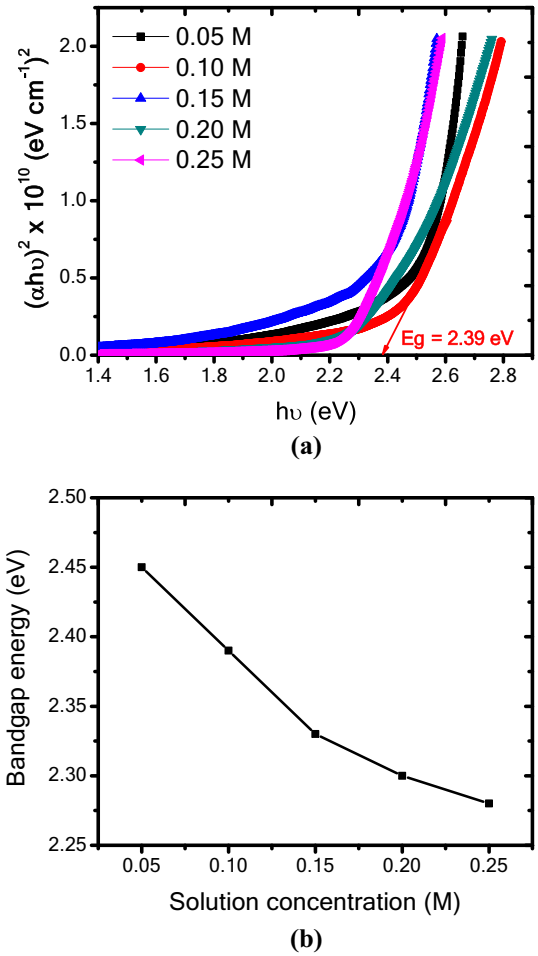

Fig. 6 **a** Plot of $(\alpha h\upsilon)^2$ against hυ and **b** variation of bandgap energy with precursor solution concentration for $CoFe_2O_4$ thin films prepared by spray pyrolysis

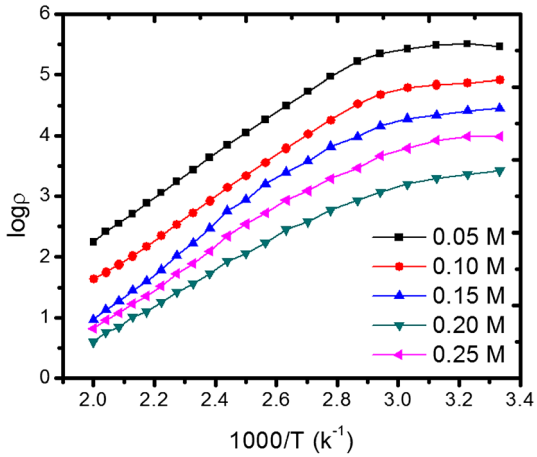

Fig. 7 Plot logρ versus inverse of absolute temperature (1000/T) for $CoFe_2O_4$ thin films prepared by spray pyrolysis with various precursor solution concentrations

3.7 Electrochemical characterization

3.7.1 *Cyclic voltammetry*

CV is a powerful electrochemical technique generally employed to examine the reduction and oxidation processes of molecular species [37]. The electrochemical performance of $CoFe_2O_4$ thin films prepared by spray pyrolysis with various precursor solution concentrations was studied using the CV tool in 1 M KOH electrolyte within potential window 0.0 to 0.55 V versus Ag/AgCl. Figure 8 shows CV curves at different scan rates for $CoFe_2O_4$ thin films prepared by spray pyrolysis with various precursor solution concentrations. All CV curves show the oxidation–reduction peaks during the cathodic and anodic sweeps indicating pseudocapacitive behaviour [38] of $CoFe_2O_4$ thin film electrodes. Figure 9a shows the CV curves at scan rate of 10 mVs^{-1} for $CoFe_2O_4$ thin film electrodes. It was observed that area under the CV curve increases with increase in solution concentration upto 0.20 M and decreases thereafter.

The specific capacitances at different scan rates were determined using the relation given elsewhere [39] and are listed in Table 4. Specific capacitance increases with increase in precursor solution concentration reaching maximum 593 Fg^{-1} at scan rate of 5 mVs^{-1} for $CoFe_2O_4$ thin film prepared with 0.20 M solution concentration and decreases thereafter for

Table 3 Optical and electrical properties of $CoFe_2O_4$ thin films prepared by spray pyrolysis with various precursor solution concentrations

Solution Conc. (M)	Optical bandgap (eV)	Electrical resistivity (Ωcm)		Activation energy (eV)	
		300 K (× 10^3)	500 K (× 10^1)	LT	HT
0.05	2.45	288	17.78	0.002	0.049
0.10	2.39	83.2	4.365	0.006	0.041
0.15	2.33	28.2	0.933	0.008	0.051
0.20	2.30	2.63	0.398	0.010	0.045
0.25	2.28	9.77	0.667	0.009	0.044

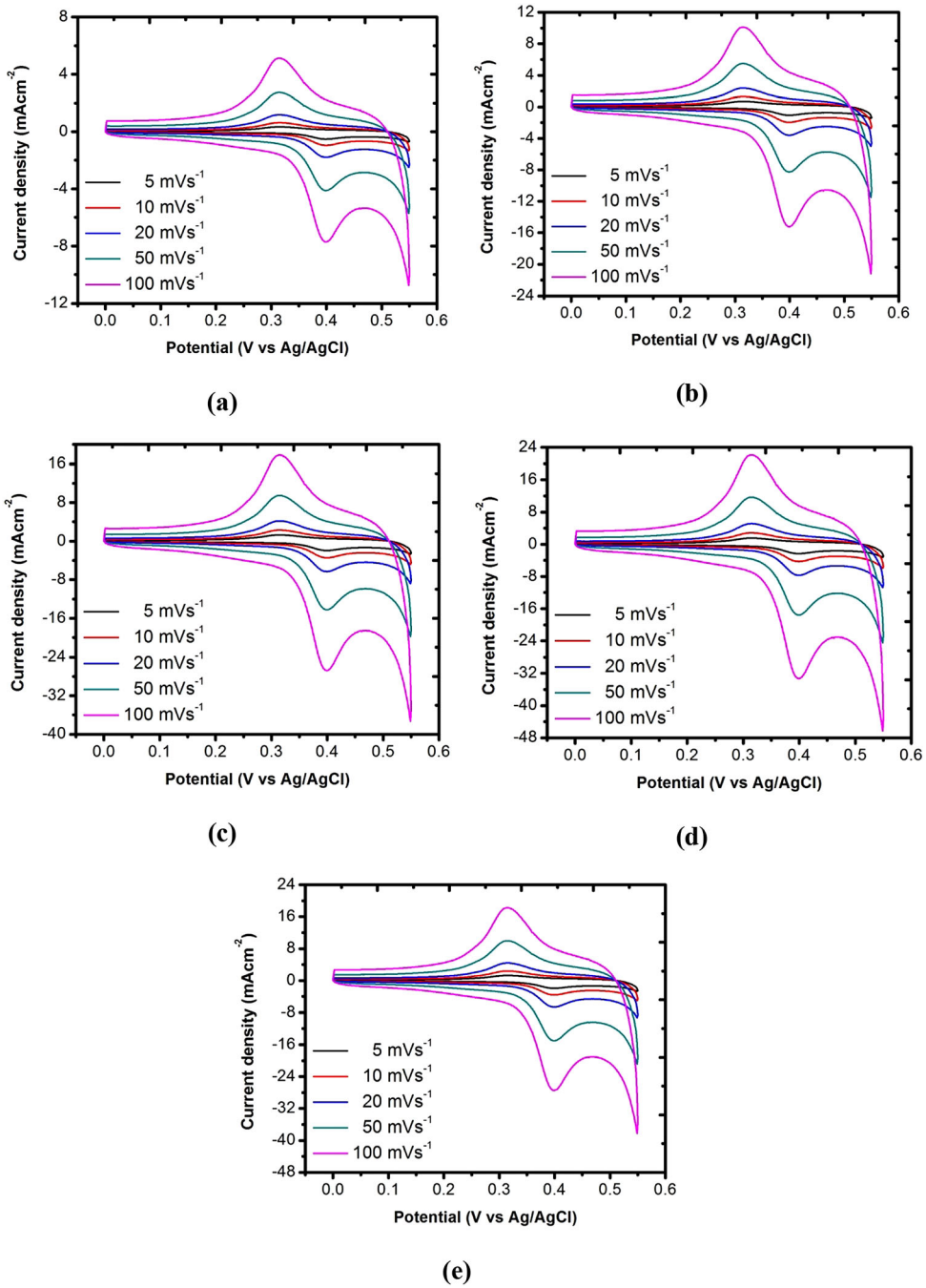

Fig. 8 CV curves at different scan rates for $CoFe_2O_4$ thin films prepared by spray pyrolysis with precursor solution concentrations of **a** 0.05 M, **b** 0.10 M, **c** 0.15 M, **d** 0.20 M and **e** 0.25 M, respectively

further increase in solution concentration. This is because $CoFe_2O_4$ thin film prepared with 0.20 M solution concentration has better crystallinity and surface morphology providing easier ionic intercalation/deintercalation [40, 41]. The specific capacitance of 593 Fg^{-1} at scan rate of 5 mVs^{-1} observed in present study is higher than 254 Fg^{-1} at scan rate 10 mVs^{-1} reported by Ahmadi and colleagues for $CoFe_2O_4$ prepared by microwave assisted auto combustion method [42], 235 Fg^{-1} for $CoFe_2O_4$-graphene composite reported by Lee et al. [43] by aerosol spray pyrolysis and is comparable with 600 Fg^{-1} for $CoFe_2O_4$@carbon sphere electrode prepared by one step solvothermal method [44].

Figure 9b shows the plot of specific capacitance versus scan rate for $CoFe_2O_4$ thin film prepared by spray pyrolysis with various precursor solution concentrations. The specific capacitance decreases

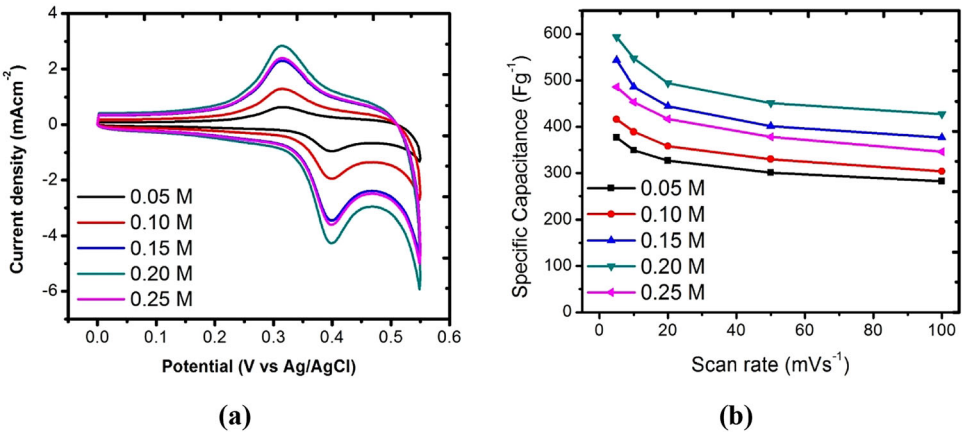

(a) (b)

Fig. 9 **a** CV plots at scan rate of 10 mVs^{-1} for comparison and **b** plot of specific capacitance versus scan rate for $CoFe_2O_4$ thin film electrodes prepared by spray pyrolysis with various precursor solution concentrations

Table 4 Specific capacitance from CV for $CoFe_2O_4$ thin film electrodes prepared by spray pyrolysis with various precursor solution concentrations

Solution concentration (M) → Scan rate (mVs^{-1}) ↓	0.05	0.10	0.15	0.20	0.25
	Specific capacitance from CV (Fg^{-1})				
5	377	416	543	593	486
10	349	389	486	547	453
20	327	358	444	494	417
50	301	330	401	451	378
100	282	304	377	427	346

with increase in scan rate due to existence of inner active sites, which cannot perform redox transition completely at higher scan rates, whereas at lower scan rates, inner and outer pores of $CoFe_2O_4$ are available for ion diffusion hence more charge is stored resulting in maximum specific capacitance [40].

3.7.2 *Galvanostatic charge–discharge*

Galvanostatic charge–discharge (GCD) measurements $CoFe_2O_4$ thin film electrodes prepared by spray pyrolysis with various solution concentrations were carried out at different current densities ranging from 0.5–4.0 Ag^{-1} in a steady potential window of 0.0 V to 0.55 V and are shown in Fig. 10. GCD measurements show linear behavior up to a maximum voltage of 0.55 V demonstrating the typical ideal capacitive behavior. From figure, it is clear that as current density of the $CoFe_2O_4$ thin film electrode increases the charge–discharge time decreases due to slow and irreversible faradaic reaction during redox mechanism [45].

Figure 11a shows the GCD curves at current density of 1 Ag^{-1} for $CoFe_2O_4$ thin film electrodes prepared by spray pyrolysis with various precursor solution concentrations. The charge–discharge curve shows the pseudocapacitive behaviour of the $CoFe_2O_4$ thin film electrodes due to redox reaction [46, 47]. The specific capacitance, specific energy and specific power for $CoFe_2O_4$ thin film electrodes at various solution concentrations were calculated using the equation given in literature [48] and are listed in Table 5.

As solution concentration used for preparation of $CoFe_2O_4$ thin film increases from 0.05 M to 0.20 M, the specific capacitance at current density of 0.5 Ag^{-1} increases from 399 Fg^{-1} to 628 Fg^{-1} and for further increase in precursor solution concentration from 0.20 M to 0.25 M the specific capacitance decreases to 515 Fg^{-1}. This behaviour can be related to the better crystallinity and porous morphology observed for $CoFe_2O_4$ thin film prepared at 0.20 M precursor solution concentration from XRD and FESEM. The specific capacitance values obtained from GCD are higher than obtained from CV because the specific capacitance calculations from GCD and CV have their typical point of dependence factors. Most of the researchers consider the GCD as the technique of choice for varying reasons. The specific capacitance obtained from GCD depends on current density, whereas specific capacitance obtained from CV depends on scan rate. These values of specific

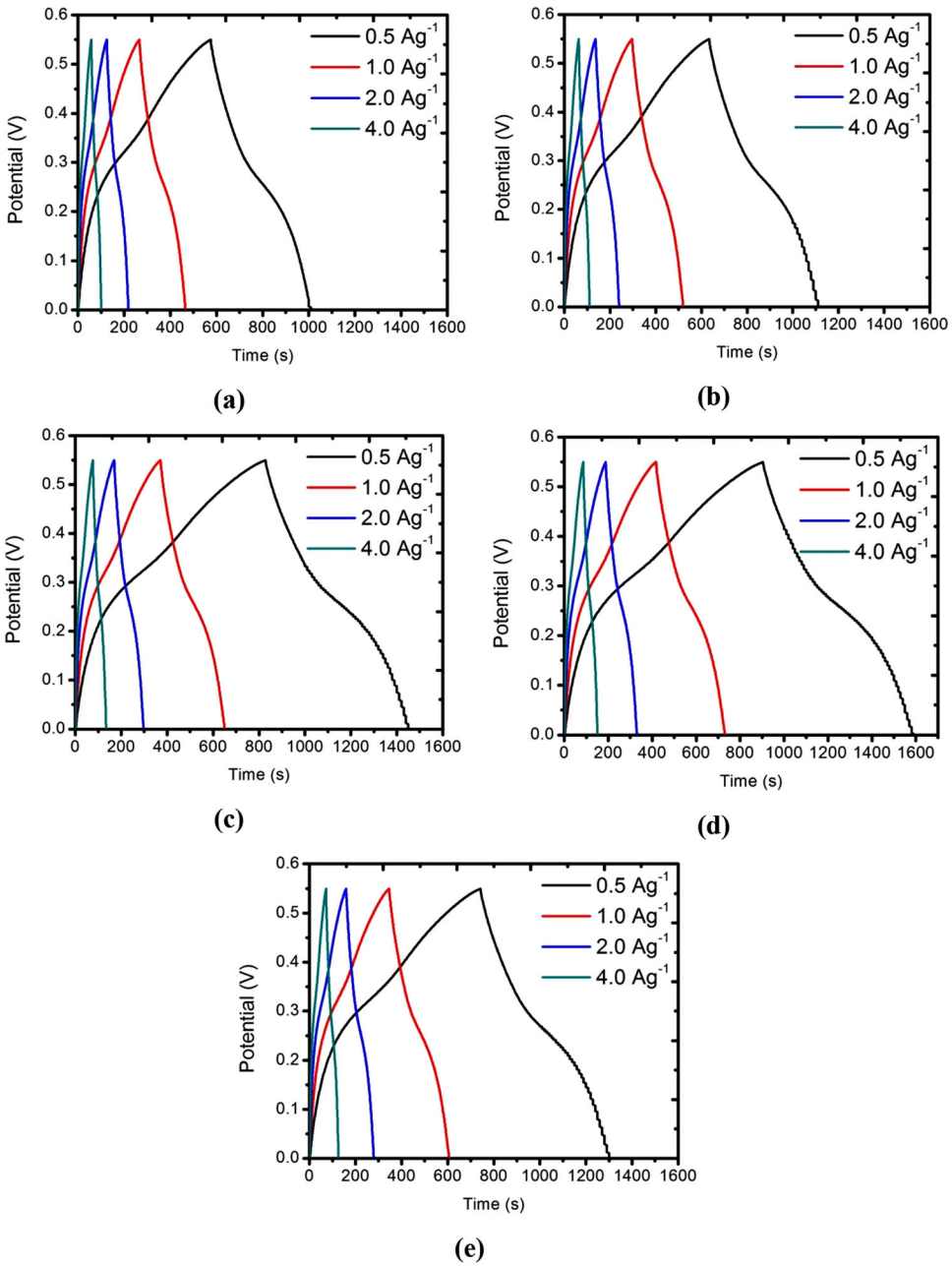

Fig. 10 GCD curves at different current densities for $CoFe_2O_4$ thin film electrodes prepared by spray pyrolysis with precursor solution concentrations of **a** 0.05 M, **b** 0.10 M, **c** 0.15 M, **d** 0.20 M and **e** 0.25 M, respectively

capacitances are higher than 18.7 Fg^{-1} at current density of 5 mAg^{-1} reported by He et al. [49] for Graphene Oxide-$CoFe_2O_4$ composites prepared by coprecipitation method and 39.4 Fg^{-1} at current density of 0.1 Ag^{-1} reported by Xiong and colleagues [50] for cobalt ferrite nanocomposites.

Figure 11b shows variation of specific capacitance with current density for $CoFe_2O_4$ thin films prepared by spray pyrolysis with various precursor solution concentrations. The specific capacitance of the $CoFe_2O_4$ thin film electrode decreases with increase in current density because at lower current density the film surface area is sufficient for the access of electrolyte ions [48]. Figure 11c shows the Ragone plot of $CoFe_2O_4$ thin film prepared with 0.20 M precursor solution concentration. Table 6 shows the specific energy and specific power for $CoFe_2O_4$ thin film prepared by spray pyrolysis with 0.20 M precursor solution concentration. The specific energy and specific power are found to be 20.08 $Whkg^{-1}$ and 1100 Wkg^{-1} respectively at current density of 4 Ag^{-1}. The long term cycle stability of $CoFe_2O_4$ thin film is

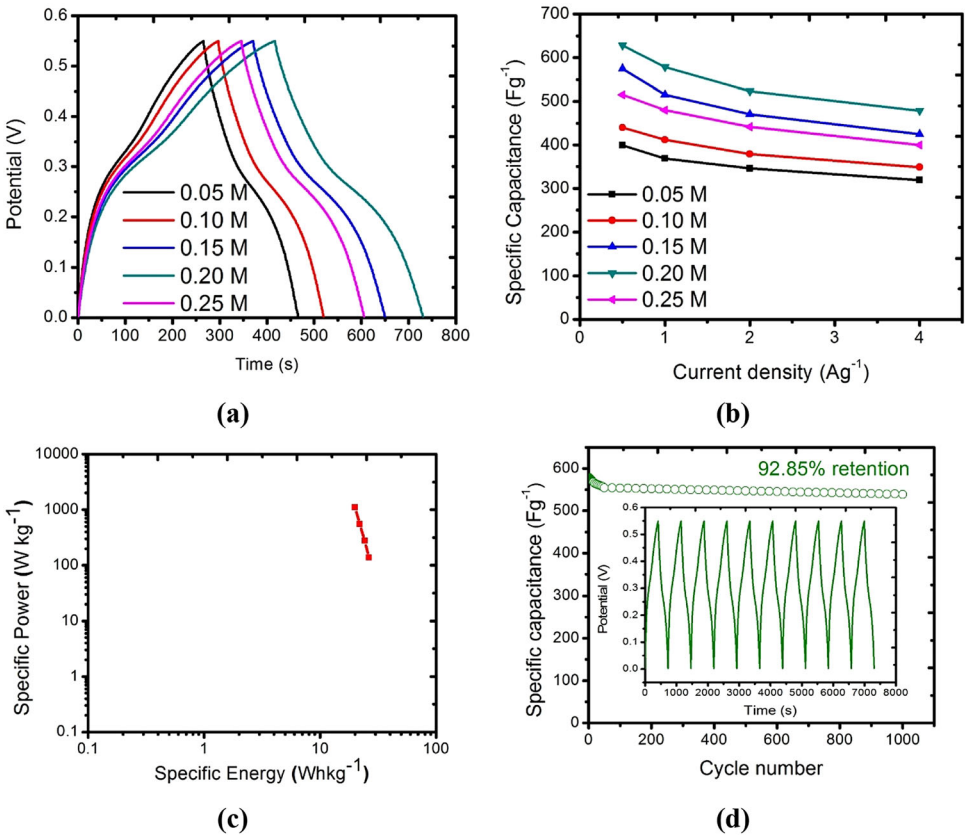

Fig. 11 **a** GCD curves at current density of 1 Ag^{-1}, **b** Variation of specific capacitance versus current density for $CoFe_2O_4$ electrodes prepared by spray pyrolysis with various precursor solution concentrations, **c** Ragone plot of $CoFe_2O_4$ electrode prepared with 0.20 M precursor solution concentration, and **d** Long term cycling performance of the 0.20 M $CoFe_2O_4$ electrode at 1 Ag^{-1}. The inset shows the charge–discharge curves of the first 10 cycles

Table 5 Specific capacitance from GCD studies for $CoFe_2O_4$ thin film electrodes prepared by spray pyrolysis with various precursor solution concentrations

Solution concentration (M) → Current density (Ag^{-1}) ↓	0.05	0.10	0.15	0.20	0.25
	Specific capacitance from GCD (Fg^{-1})				
0.5	399	440	575	628	515
1	369	412	515	579	480
2	346	379	470	523	442
4	319	349	425	478	400

crucial parameter for practical applications. The cycle performance of $CoFe_2O_4$ electrode prepared by spray pyrolysis with 0.20 M precursor solution concentration was studied at current density of 1 Ag^{-1} and is shown in Fig. 11d. After the 1000 charge–discharge cycles, the specific capacitance of $CoFe_2O_4$ thin film electrode maintains 92.85% of its initial value, indicating the good electrochemical cycle stability and reversibility of the material.

3.7.3 *Electrochemical impedance spectroscopy*

The impedance spectra were measured in the frequency range of 1 to 100,000 Hz in 1 M KOH electrolyte solution. Figure 12 shows the Nyquist plots

Table 6 The specific energy (SE) and specific power (SP) for $CoFe_2O_4$ thin film electrodes prepared by spray pyrolysis with 0.20 M precursor solution concentration

Current density (Ag^{-1})	Discharge time (s)	SE ($Whkg^{-1}$)	SP (Wkg^{-1})
0.5	691	26.38	138
1	318	24.33	275
2	144	21.97	550
4	66	20.08	1100

for of $CoFe_2O_4$ thin film electrodes prepared by spray pyrolysis with various solution concentrations. The values of Rs and Rct obtained from the EIS investigation are listed in Table 7. It is found that the minimum solution resistance (Rs) was 0.18 Ω and charge transfer resistance (Rct) was 13.05 Ωcm^2 for $CoFe_2O_4$ thin film electrode prepared by spray pyrolysis with 0.20 M solution concentration. The minimum resistance observed for $CoFe_2O_4$ thin film electrode prepared 0.20 M solution concentration provides more access of electrolyte ions to the surface and reduces the ion diffusion path showing better electrochemical performance.

4 Conclusions

Precursor solution concentration dependent $CoFe_2O_4$ thin film electrodes are prepared using chemical spray pyrolysis technique. The increase in solution concentration upto 0.20 M was found to improve the specific capacitance (593 Fg^{-1} in 5 mVs^{-1} from CV and 628 Fg^{-1} at a current density of 0.5 Ag^{-1} from GCD), cycle life (92.85% capacitance retention after 1000 cycles) due to their mesoporous morphology, rapid ionic transport and accessible electrochemically reactive sites. The $CoFe_2O_4$ thin film electrodes exhibited specific energy of 21.97 $Whkg^{-1}$ and specific power of 550 Wkg^{-1} at current density of 2 Ag^{-1} comparable to the start-of-the-art values reported in the literature. The variation in precursor solution concentration provided a platform to improve morphology and electrical conductivity.

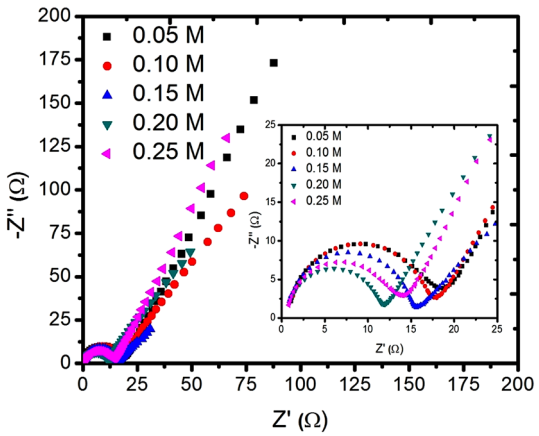

Fig. 12 Nyquist plot for $CoFe_2O_4$ thin film electrodes prepared by spray pyrolysis with various precursor solution concentrations

Table 7 Nyquist data for $CoFe_2O_4$ thin film electrodes prepared by spray pyrolysis with various solution concentrations

Solution concentration (M)	Rs (Ω)	Rct (Ω cm^2)
0.05	0.40	22.25
0.10	0.30	18.75
0.15	0.25	16.15
0.20	0.18	13.05
0.25	0.21	15.30

Author contributions

All authors contributed to the study conception and design. Material preparation, data collection and analysis were performed by all authors. The first draft of the manuscript was written by VJ and AY commented on previous versions of the manuscript. All authors read and approved the final manuscript.

Data availability

It is hereby assured that materials described in the manuscript, including all relevant raw data, will be freely available to any researcher wishing to use them for non-commercial purposes, without breaching participant confidentiality.

Declarations

Conflict of interest There are no financial or non-financial interests. There is no conflict to declare.

Ethical approval This article does not contain any studies with human or animal subjects.

References

1. M. Geerthana, S. Prabhu, S. Harish, M. Navaneethan, R. Ramesh, M. Selvaraj, Design and preparation of ternary α-Fe_2O_3/SnO_2/rGO nanocomposite as an electrode material for supercapacitor. J. Mater. Sci.: Mater. Electron. **33**, 8327–8343 (2022)
2. S. Elumalai Dhandapani, N.D. Prabhu, R. Ramesh, Bifunctional copper zinc bimetallic tungstate nanoparticles decorated reduced graphene oxide (CuZnWO4/rGO) for high-performance photocatalytic and supercapacitor application. J. Mater. Sci.: Mater. Electron. **33**, 8446–8459 (2022)

3. B. Al-Najar, A. Younis, L. Hazeem, S. Sehar, M. Suad Rashdan, N. Shaikh, H. Albuflasa, N.P. Hankins, Thermally induced oxygen related defects in eco-friendly $ZnFe_2O_4$ nanoparticles for enhanced wastewater treatment efficiencies. Chemosphere **288**, 132525 (2022)
4. M. Koç, Ç.E.D. Dönmez, L. Paralı, A. Sarı, S. Aktürk, Piezoelectric and magnetoelectric evaluations on PVDF/$CoFe_2O_4$ based flexible nanogenerators for energy harvesting applications. J Mater Sci: Mater Electron **33**, 8048–8064 (2022)
5. S. Anjum, G.H. Jaffar, A.K. Rumaiz, M.S. Rafique, S.I. Shah, Role of vacancies in transport and magnetic properties of nickel ferrite thin films. J. Phys. D: Appl. Phys. **43**, 265001 (2010)
6. Q. Wang, H. Gao, X. Qin, J. Dai, W. Li, Fabrication of $NiFe_2O_4$@$CoFe_2O_4$ core-shell nanofibers for high performance supercapacitors. Mater. Res. Express **7**, 015020 (2020)
7. S.M. Bououdina, C. Manoharan, Dependence of structure/morphology on electrical/magnetic properties of hydrothermally synthesized cobalt ferrite nanoparticles. J. Magn. Magn. Mater. **493**, 165703 (2020)
8. A. Shabani, G. Nabiyouni, D. Ghanbari, Preparation and photocatalytic study of $CoFe_2O_4$/TiO_2/Au nanocomposites and their applications in organic pollutant degradation and modeling by an artificial neural network (ANN). J. Mater. Sci.: Mater. Electron. **33**, 9885–9904 (2022)
9. N. Labchir, A. Hannour, A. Ait Hssi, D. Vincent, A. Soussi, A. Ihlal, Facile galvanostatic electrodeposition of $CoFe_2O_4$ nanosheets from sulfate medium. J. Mater. Sci.: Mater. Electron. **32**, 27987–27994 (2021)
10. J. Sagu, D. Mehta, K. Wijayantha, Electrocatalytic activity of $CoFe_2O_4$ thin films prepared by AACVD towards the oxygen evolution reaction in alkaline media. Electrochem. Comm. **87**, 1–4 (2018)
11. B. Yalcin, S. Ozcelik, K. Icin, K. Senturk, B. Ozcelik, L. Arda, Structural, optical, magnetic, photocatalytic activity and related biological effects of $CoFe_2O_4$ ferrite nanoparticles. J. Mater. Sci: Mater. Electron. **32**, 13068–13080 (2021)
12. S. Sathaye, K. Patil, S. Kulkarni, P. Bakre, S. Pradhan, B. Sarwade, S. Shintre, Modification of spin coating method and its application to grow thin films of cobalt ferrite. J. Mater. Sci. **38**, 29–33 (2003)
13. D. Kshamitha, V. Manjunath, S. Dastagiri, P. Reddy Prasad, M.V. Lakshmaiah, S. Afr. J. Chem. Eng. **33**, 51–57 (2020)
14. J.S. Sagu, K.G.U. Wijayantha, A.A. Tahir, The Pseudocapacitive nature of $CoFe_2O_4$ Thin Films. Electrochim. Acta **246**, 870–878 (2017)
15. A.A Bagade, V.V. Ganbavle , S.V. Mohite, T.D. Dongale, B.B. Sinha, K.Y. Rajpure (2017) Assessment of structural, morphological, magnetic and gas sensing properties of $CoFe_2O_4$ thin films. J. Coll. Interf. Sci. 181–192
16. C. Falcony, M.A. Aguilar-Frutis, M. García-Hipólito, Spray pyrolysis technique; high-K dielectric films and luminescent materials: A review. Micromachines **9**, 414 (2018)
17. S. Kozhukharov, S. Tchaoushev, Spray pyrolysis equipment for various applications. J. Chem. Technol. Metall. **48**, 111–118 (2013)
18. A.A. Yadav, U.J. Chavan, Electrochemical supercapacitive performance of spray-deposited NiO electrodes. J. Electron. Mater. **47**(7), 3770–3778 (2018)
19. JCPDS data card (22–1086).
20. A.R. Babar, S.S. Shinde, A.V. Moholkar, C.H. Bhosale, J.H. Kim, K.Y. Rajpure, Sensing properties of sprayed antimony doped tin oxide thin films: Solution molarity. J. Alloys Compd. **509**(6), 3108–3115 (2011)
21. Y. Zhang, A. Sun, L. Shao, Z. Suonan, J. Chen, Structural, magnetic, optical, and impedance properties of $Sr_xCo_{1-x}Fe_2O_4$ nanoparticles prepared by sol–gel method. J Mater Sci: Mater Electron **32**, 21262–21277 (2021)
22. M. Bouderbala, S. Hamzaoui, B. Amrani, A.H. Reshak, M. Adnane, T. Sahraoui, M. Zerdali, Thickness dependence of structural, electrical and optical behaviour of undoped ZnO thin films. Phys. B **403**, 3326–3330 (2008)
23. C.D. Lokhande, A.U. Ubale, P.S. Patil, Thickness dependent properties of chemically deposited Bi_2S_3 thin films. Thin Solid Films **302**(1–2), 1–4 (1997)
24. A.A. Bagade, K.Y. Rajpure, Development of $CoFe_2O_4$ thin films for nitrogen dioxide sensing at moderate operating temperature. J. Alloys Compd. **657**, 414–421 (2016)
25. M.P. Reddy, A.M.A. Mohamed, X.B. Zhou, S. Du, Q. Huang, A facile hydrothermal synthesis, characterization and magnetic properties of mesoporous $CoFe_2O_4$ nanospheres. J. Magn. Magn. Mater. **388**, 40–44 (2015)
26. T. Shang, Q. Lu, L. Chao, Y. Qin, Y. Yun, G. Yun, Effects of ordered mesoporous structure and La-doping on the microwave absorbing properties of $CoFe_2O_4$. Appl. Surf. Sci. **434**, 234–242 (2018)
27. Zu. Lianhai, W. Zhang, Qu. Longbing, L. Liu, W. Li, Yu. Aibing, D. Zhao, Mesoporous materials for electrochemical energy storage and conversion. Adv. Energy Mater. **10**, 2002152 (2020)
28. A. Kalam, A.G. Al-Sehemi, M.D.G. Assiri, T. Ahmad, I. Ahmad, M. Pannipara, Modified solvothermal synthesis of cobalt ferrite ($CoFe_2O_4$) magnetic nanoparticles photocatalysts for degradation of methylene blue with H_2O_2 /visible light. Results Phys. **8**, 1046–1053 (2018)
29. A.V. Ravindra, P. Padhan, W. Prellier, Electronic structure and optical band gap of $CoFe_2O_4$ thin films. Appl. Phys. Lett. **101**(16), 161902 (2012)

30. N.T.T. Loan, N.T.H. Lan, N.T.T. Hang, N.Q. Hai, D.T.T. Anh, V.T. Hau, L.V. Tan, T.V. Tran, $CoFe_2O_4$ nanomaterials: effect of annealing temperature on characterization. Magnetic, Photocatalytic, and Photo-Fenton Properties, Processes **7**, 885 (2019)
31. D. Yuliantika, A. Taufiq, A.H. Sunaryono, N. Hidayat, S. Soontaranon, Exploring structural properties of cobalt ferrite nanoparticles from natural sand. IOP: Conf. Ser. Mater. Sci. Eng. **15**, 0120 (2019)
32. A.A. Bagade, V.V. Ganbavle, K.Y. Rajpure, Physicochemical properties of spray-deposited $CoFe_2O_4$ thin films. J. Mater. Eng. Perform. **23**(8), 2787–2794 (2014)
33. A.A. Yadav, Spray deposition of tin oxide thin films for supercapacitor applications: Effect of solution molarity. J. Mater. Sci. Mater. **27**(7), 6985–6991 (2016)
34. A.A. Yadav, Influence of film thickness on structural, optical, and electrical properties of spray deposited antimony doped SnO_2 thin films. Thin Solid Films **591**, 18–24 (2015)
35. A. Chapelle, F. Oudrhiri-Hassani, L. Presmanes, A. Barnab, P. Tailhades, CO_2 sensing properties of semiconducting copper oxide and spinel ferrite nanocomposite thin film. Appl. Surf. Sci. **256**, 4715–4719 (2010)
36. A.B. Shinde, Structural and electrical properties of cobalt ferrite nanoparticles. IJITEE **3**(4), 64–67 (2013)
37. A. Younis, D. Chu, Abdul Hadi Shah, Haiwei Du, Sean Li, interfacial redox reactions associated ionic transport in oxide-based memories. ACS Appl. Mater. Interfaces **9**, 1585–1592 (2017)
38. K. Sathiyamurthy, C. Rajeevgandhi, L. Guganathan, S. Bharanidharan, S. Savithiri, Enhancement of magnetic, supercapacitor applications and theoretical approach on cobalt-doped zinc ferrite nanocomposites. J. Mater. Sci. Mater. Electron. **32**(9), 11593–11606 (2021)
39. A. Robert Xavier, A.T. Ravichandran, M. Subbukalai Vijayakumar, S. Dhivya Angelin, J.P. Rajkumar, Merlin, Synthesis and characterization of Sr-doped CdO nanoplatelets for supercapacitor applications. J. Mater. Sci.: Mater. Electron. **33**, 8426–8434 (2022)
40. N. Kumar, A. Kumar, G.-M. Huang, Wu. Wen-Wei, T.Y. Tseng, Facile synthesis of mesoporous $NiFe_2O_4$/CNTs nanocomposite cathode material for high performance asymmetric pseudocapacitors. Appl. Surf. Sci. **433**, 1100–1112 (2018)
41. A.A. Yadav, U.J. Chavan, Electrochemical supercapacitive performance of spray deposited Co_3O_4 thin film Nanostructures. Electrochim. Acta **232**, 370–376 (2017)
42. R. Ahmadi, M. Imani, A. Tadjarodi, Microwave assisted synthesis of $CoFe_2O_4$ nanoparticles by utilizing organic promoters and evaluation of its properties, properties. Chem. Proc. **3**, 52 (2021)
43. C. Lee, H. Chang, H.D. Jang, Preparation of $CoFe_2O_4$-graphene composites using aerosol spray pyrolysis for supercapacitors application. Aerosol. Air Qual. Res. **19**, 443–448 (2019)
44. A.M. Elseman, M.G. Fayed, S.G. Mohamed, D.A. Rayan, N.K. Allam, M.M. Rashad, Q. Song, A novel composite $CoFe_2O_4$@CSs as electrode by easy one-step solvothermal for enhancing the electrochemical performance of hybrid supercapacitors. Chem. Electro. Chem. **7**, 526–534 (2020)
45. W. Yao, L. Li, Z. Bai, Y. Jiang, L. Xu, J. Yan, Y. Wan, R. Tan, H. Liu, P. Liu, Effect of graphene quantum dots on the capacitance performances of flexible PEDOT: PSS films. Int. J. Electrochem. Sci. **15**, 9135–9145 (2020)
46. B.Y. Fugare, B.J. Lokhande, Study on structural, morphological, electrochemical and corrosion properties of mesoporous RuO_2 thin films prepared by ultrasonic spray pyrolysis for supercapacitor electrode application. Mater. Sci. Semicond Process. **71**, 121–127 (2017)
47. S. Teng, G. Siege, W. Wang, A. Tiwari, Carbonized wood for supercapacitor electrodes. ECS Solid State Lett. **3**(5), M25–M28 (2014)
48. M. Gupta, S. Tyagi, N. Kumari, Electrochemical evaluation of highly stable Mn ferrite/PEDOT/rGO ternary nanocomposite for supercapacitor electrodes. J. Mater. Sci: Mater. Electron. **33**, 7838–7852 (2022)
49. P. He, K. Yang, W. Wang, F. Don, L. Du, Y. Deng, Reduced graphene oxide-$CoFe_2O_4$ composites for supercapacitor electrode. Russ. J. Electro chem **49**(4), 359–364 (2013)
50. P. Xiong, H. Huang, X. Wang, Design and synthesis of ternary cobalt ferrite/graphene/polyaniline hierarchical nanocomposites for high-performance supercapacitors. J. Power Sources **245**, 937–946 (2014)